Monica Y. Oña Vera, Giovanni Metelli, Joaquim Barros, Giovanni Plizzari

EFFECTS OF NEW OPENINGS ON THE IN-PLANE BEHAVIOR OF UNREINFORCED BRICK MASONRY WALLS

Mónica Y. Oña Vera[1]**, Giovanni Metelli**[1]**, Joaquim A. O. Barros** [2]**, Giovanni Plizzari**[1]

[1] Department of Civil, Environmental, Architectural Engineering and Mathematics. University of Brescia, Via Branze 43, Brescia, Italy.
e-mail: m.onavera@unibs.it, giovanni.metelli@unibs.it, giovanni.plizzari@unibs.it

[2] Department of Civil Engineering, University of Minho, Campus de Azurém, 4800-058, Guimaraes, Portugal, email: barros@civil.uminho.pt,

Keywords: Openings, in-plane behavior, modeling, cyclic test

Abstract. *Existing brick masonry buildings are frequently modified to satisfy nowadays living demands. Such modifications may include new windows or doors that connect two rooms and require openings to be cut from load bearing walls. In current design practice, these interventions are generally designed and verified for vertical load, but the structural behavior of these altered walls when submitted to in-plane loads (due to seismic actions) is not yet fully understood. Thus, design practice may be inaccurately estimated. The objective of this work is to evaluate, numerically and experimentally, the effects of introducing openings in masonry solid-brick walls subjected to in-plane loading. Three main parameters are considered for the numerical studies: i) walls dimensions, ii) opening type, iii) opening size. As expected, results show that walls with medium-large openings are the most vulnerable case-scenario. These numerical results have addressed the design of a representative wall tested at the University of Brescia. The preliminary results of this experimental program are included in this paper.*

1 INTRODUCTION

The use of fired clay bricks masonry is particularly common in flat areas of the Center and North of Italy, where clay is largely available and is one of the main construction material for modern buildings built before the Seismic Design became mandatory for this region. These types of existing buildings often require upgrades or interventions to conform owners with new living demands. Common requests may include cutting-out new doors to connect two adjacent rooms or to create the entrance of a new garage (Figure 1). The latter is a typical intervention in the historical centers of many cities in Italy. Smaller openings for windows or ventilation paths are often requested as well, especially in ground floor buildings which can be transformed to a shop or showroom. Current Italian and European standards suggest that these types of interventions should be, if possible, avoided for unreinforced masonry buildings, to minimize unfavorable effects of structural discontinuity and irregularity. New openings could be a source of weakness and can size-dependently reduce the structures' stiffness and change its seismic performance.

a)   b)
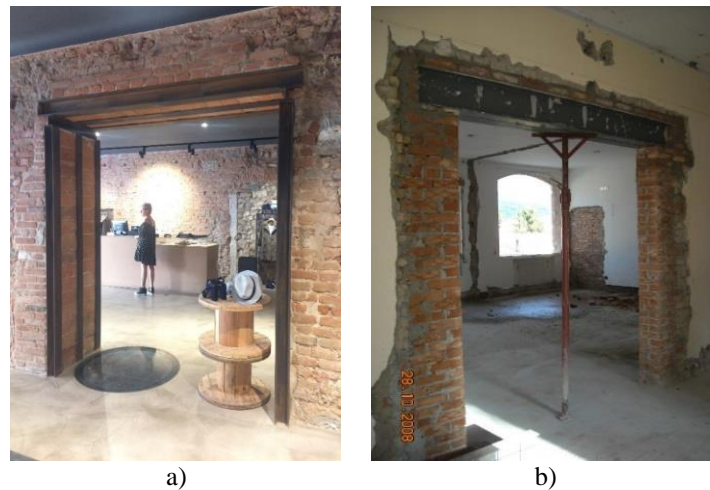
Figure 1: a) Example of a new opening in a store in the historical center of Brescia, Italy; b) new opening in the ground floor of a dwelling house.

This paper deals with the numerical evaluation of clay masonry walls with different geometry and sizes of openings for assessing the effects of new discontinuities in load bearing walls when an in-plane seismic action is applied. The numerical analyses were carried out in order to provide valuable information for the design of a wall specimen type to be constructed as a solid wall, then perforated and tested under in-plane load.

Preliminary results from the in-plane test on a masonry wall with an opening intervention are also presented and compared with numerical estimates. The paper includes a short description of the cutting-out process in the chosen masonry wall specimen while constant vertical load is applied which can be representative of the common practice carried out in Italy before the introduction of the 2003 seismic code.

2 NUMERICAL MODELS

For assessing the effects of a new opening in a real solid wall, the authors selected one of the most commonly used model for macro modelling of masonry, as in [1], [2], [3], i.e., the Total Strain Fixed Crack Model (TSFCM), available in the FE program Diana TNO [4]. This

model was selected mainly because of the limited data required. Though masonry is anisotropic, and it would be more adequate to use an anisotropic model, either micro-modelling [5], continuum based [6] or mathematically homogenized [7], due to the lack of experimental information available for all the parameters of the constitutive laws of these models, and considering the main aim of these numerical studies, the authors considered opportune the use of TSFCM for predicting the strength, load deformation response and failure mode of the type of masonry walls described in Figure 2, and then derive a funded critical opinion about its predictive performance.

For verifying the ability of this model to reproduce the overall behavior of the masonry walls, a first analysis has been done simulating a solid wall of reference (MW-R) tested in an earlier research carried out by the same research group at the University of Brescia. This work can be found in reference [8], where mechanical characterization, in-plane tests and numerical modelling using the Disturbed Stress Field Model (DSFM) are described. The material proper-ties used for the numerical model of this paper are taken from the experimental results shown in [8]; the numerical results from TSFCM were validated by comparing the overall response obtained from the DSFM model and the experimental test.

2.1 Walls geometry

The dimensions of the walls are 4.35m x 3.1m x 0.25m, representing typical walls of buildings in Italy, constructed between 1900 – 1950. However, the laboratory test set up available was designed for walls of 2.2m of maximum total height. Thus, the real geometry of walls and all openings were reduced using a scale factor of 0.70 The final dimensions, designation of walls' models and brick bond type, are shown in Figure 2 and Figure 3 respectively.
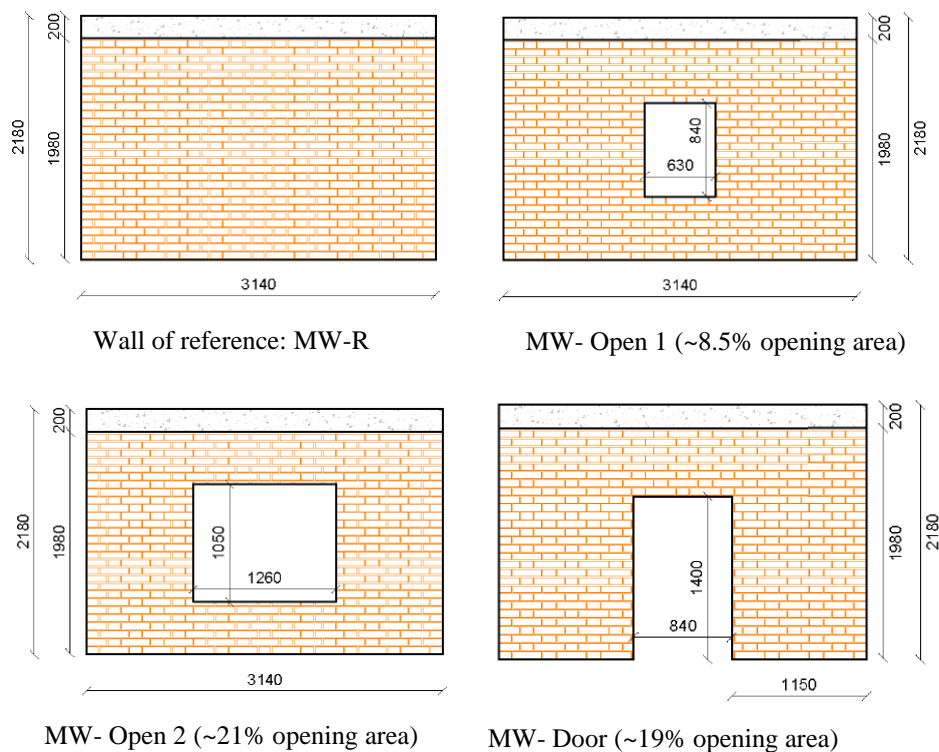

Wall of reference: MW-R

MW- Open 1 (~8.5% opening area)

MW- Open 2 (~21% opening area)

MW- Door (~19% opening area)

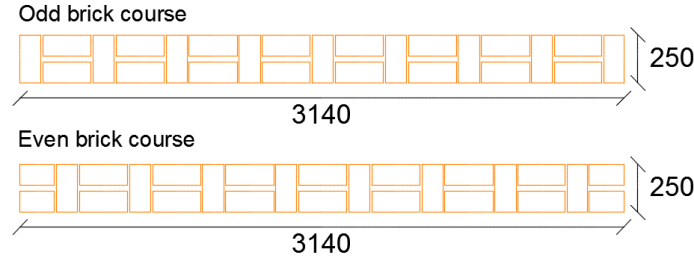Figure 2: Walls geometry. All dimensions are in [mm].

Figure 3: Brick bond pattern (Flemish bond). All dimensions are in [mm].

2.2 Material properties and constitutive relations

The inelastic deformation of the constituent materials in compression was simulated by a parabolic stress-strain relationship that includes a softening stage, while the fracture mode I propagation was modelled by the exponential curve proposed by Hordjik [9]. The crack bandwidth *h* for assuring mesh objectivity is defined as the square root of the total area of the element. The post-cracked shear stiffness, $G^{cr} = \beta G$, was simulated by using β= 0.01. The values that characterize the material properties were taken from the available experimental data and literature and are listed in Table 1.

Young Modulus*	2700 MPa
Compressive strength*	4.0 MPa
Tensile strength[++]	0.14 MPa
Compressive Fracture Energy[+]	5 N/mm
Tensile Fracture Energy[++]	0.1 N/mm

Table 1: Summary of masonry material properties validated for the numerical models.
*Parameters were taken from experimental carried out in [8].
[+]50 times the tensile fracture energy, as suggested in [4].
[++] Due to the lack of experimental data, the tensile strength and the tensile fracture energy were obtained by performing numerical inverse analysis with the experimental results of [8].

To verify the applicability of these properties in the simulations of walls from Figure 2 when using the TSFCM, the results obtained on the simulation of the MW-R were compared with the outputs from the DSFM version applied to Unreinforced Masonry, (DSFM-URM).

The major difference between the TSFCM and DSFM in the context of modelling URM is mainly restricted to the simulation of the compression behavior. The TSFCM characterizes the compression behavior by a parabolic stress-strain curve defined by the compressive strength, its corresponding strain and the energy dissipated in post-peak stage. In the case of DSFM-URM, the compressive behavior is simulated by a stress-strain relation based in a formulation proposed by Hoshikuma [10] for confined reinforced concrete. This function considers the initial elastic modulus of masonry, independently of the compressive strength and the strain at peak, the softening branch of the stress-strain relationship is provided by the modified Kent-Park model for masonry. As explained in [4] and [11], the compressive constitutive law for the TSFCM considers the material as an isotropic continuum initially developed along the lines of the Modified Compression Field Theory, originally proposed by Vecchio & Collins [12]. The DSFM-URM on the other hand is an advancement of the DSFM for reinforced concrete, specifically developed by Vecchio in 2000 [13], it is based on the Ganz failure criterion and, thus,

considers the orthotropy of masonry in compression. Further explanation about this model and its formulation is described elsewhere [14].

2.3 Mesh, constraints and loading conditions

Quadrilateral isoparametric plane stress elements (CQ16M), based on quadratic interpolation, were adopted. In the test set-up, walls were placed on a concrete slab fixed to the laboratory floor; thus, nodes at the base line are horizontally and vertically restrained. A top concrete beam that helps distributing uniformly the vertical load was modelled as well, as used in the test set-up used in [8]. Models were loaded in two phases: 1st) a distributed pressure of 0.32MPa due to a 250 kN vertical load was applied; 2nd) a monotonic increasing horizontal displacement was applied.
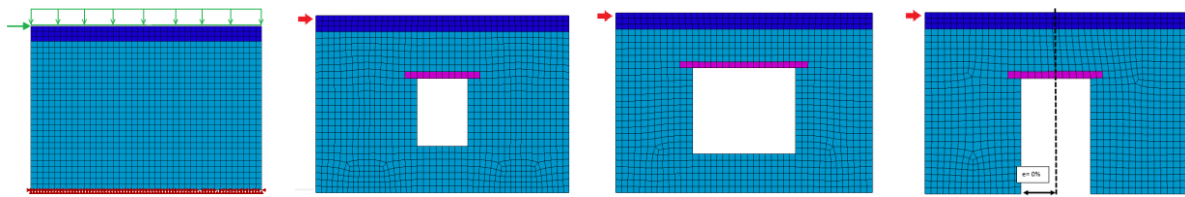

Figure 4: Left: Boundary and loading conditions for all models. Right: mesh for walls with openings.

2.4 TSFCM vs DSFM-URM for material validation

The experimental hysteretic curves envelope and the numerical response of MW-R are compared in Figure 5, where almost perfect agreement between both numerical curves can be observed. Moreover, a perfect match for the linear part of the experimental curve was found. Table 2 summarizes the peak loads and the correspondent displacements determined in the curves of Figure 5. It is verified that TSFCM differs only in 1.5% from the experimental peak load while DSFM-URM model differs in 4.2%. Figure 6 shows that the crack patterns evolution predicted by the TSFCM reproduced with fair accuracy those from the experimental test. Thus, it can be assumed that the values for model parameters indicated in Table 1 represent well the corresponding materials, regarding the prediction of the relevant behavior of this type of walls.
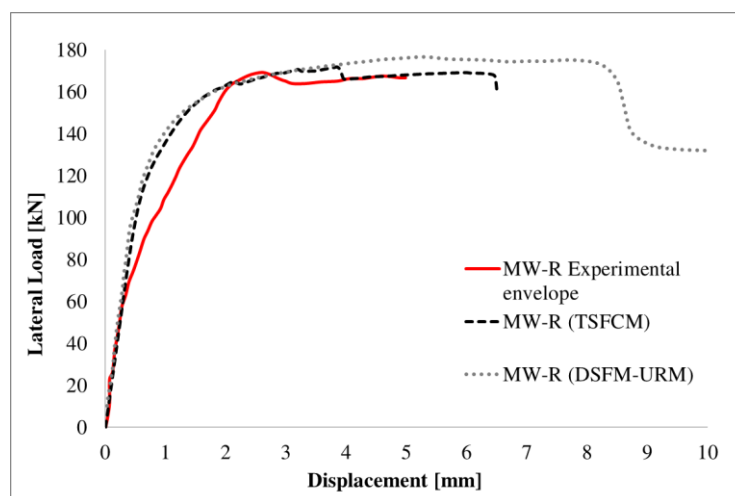

Figure 5: Comparison between experimental envelope and numerical Load – Displacement curves

	TSFCM	DSFM-URM	Experimental
Peak Load (kN)	171.99	176.79	169.32
Displacement at peak load (mm)	3.85	5.24	2.62

Table 2: Summary of peak loads obtained from L-D curves shown in Figure 6.

Figure 6 shows crack propagation patterns in terms of numerical crack width in direction X and direction Y. In the TSFCM, crack width is estimated as the product of the crack tensile strain and the crack bandwidth h. When comparing these cracks with the experimental development of cracks, good agreement between both is observed. Initially a sliding crack is developed (Crack A), followed by the formation of diagonal cracks (Crack B and Crack C) when a lateral displacement of 2.95mm was registered (drift=0.15%). These cracks evolved until the end of the test. Like observed experimentally, diagonal and sliding cracking are the main failure mechanism predicted by the numerical model.

The TSFCM was not able to fully display the right-side toe crushing until the last experimental displacement (drift 0.25%), however it was capable of capturing small flexural cracks developed on the left side of the wall.
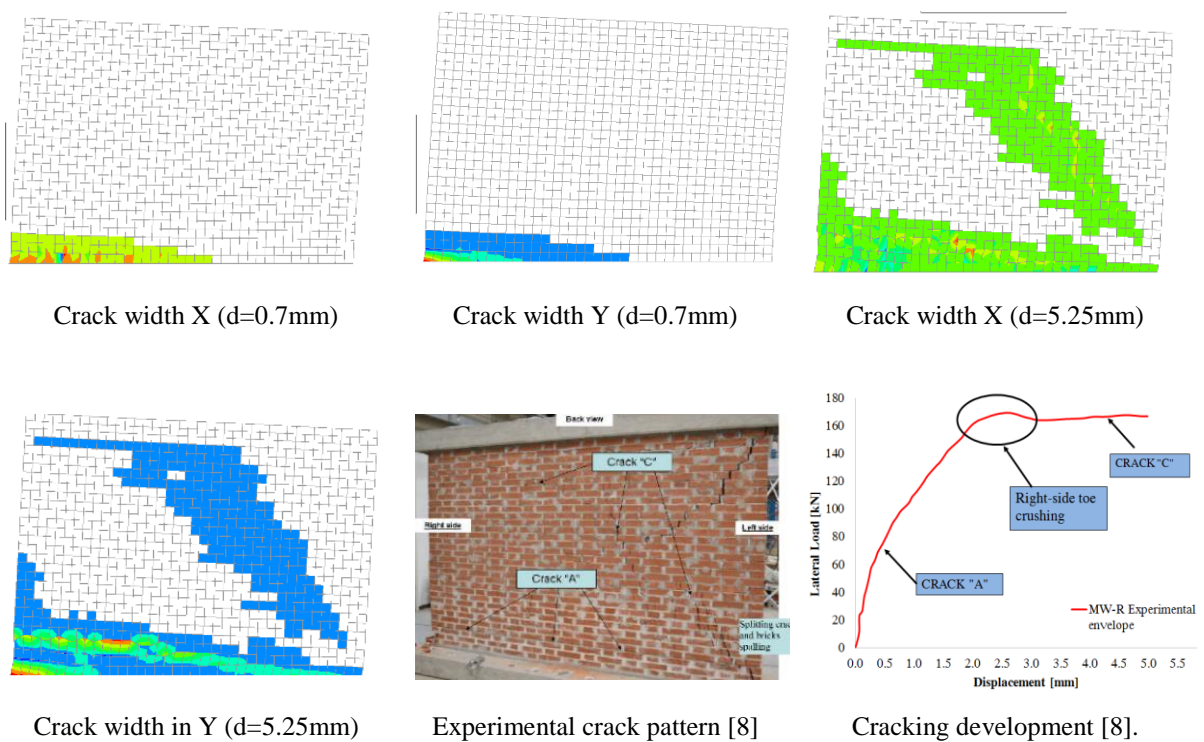

Crack width X (d=0.7mm)   Crack width Y (d=0.7mm)   Crack width X (d=5.25mm)

Crack width in Y (d=5.25mm)   Experimental crack pattern [8]   Cracking development [8].

Figure 6: Crack patterns: Numerical vs Experimental

3   NUMERICAL RESULTS

The following results are outputs from the models described in Figure 2. Material parameters, FE mesh, boundary conditions are the same as MW-R. The analyses were stopped when no

further convergence was found for small tolerances based in energy and displacement convergence (0.001 and 0.01 respectively).

3.1 MW-R vs Wall with windows

Figure 7 presents the numerical response in terms of Lateral Load – Displacement. A comparison between load carrying capacities is emphasized at a displacement of 1mm and 2mm. The wider the opening, the smaller the wall's in-plane resistance. MW-Open 2 presents a loading decay of about 40% at 2 mm of lateral displacement and an elastic stiffness reduction of about 60% with respect to the MW-R. Meanwhile MW-Open 1, has a load decay of about 15% at lateral displacement d=2mm, and a stiffness reduction of 27% with respect to MW-R.

Figure 8 shows cracking development for MW-Open 1 and MW-Open 2. For the first wall, the relevant cracking started developing at about d=1.0mm, while for the second, cracks were already formed when vertical load was applied, forming the arch shape typical of weak lintels. Final cracks for both walls are mixed: diagonal cracking along the right pier and horizontal cracking at the wall's base.

3.2 MW-Door

As shown in Figure 7, MW-Door has significantly decreased its initial stiffness in about 41% with respect to MW-R. At this loading stage there is a stress concentration in both corners of the lintel, resulting in the formation of vertical cracks in these zones. At d=1.0 mm the load carrying capacity of MW-Door 1 was 32% less than MW-R and significant cracks started developing in the spandrel and at the wall's baseline. Finally, at 2.6mm, which is the displacement at which the experimental MW-R had reached its peak load, the load carrying capacity of the MW-Door 1 was less than MW-R in about 29%. Above this load, the numerical model has shown the development of some diagonal cracks (Figure 9).
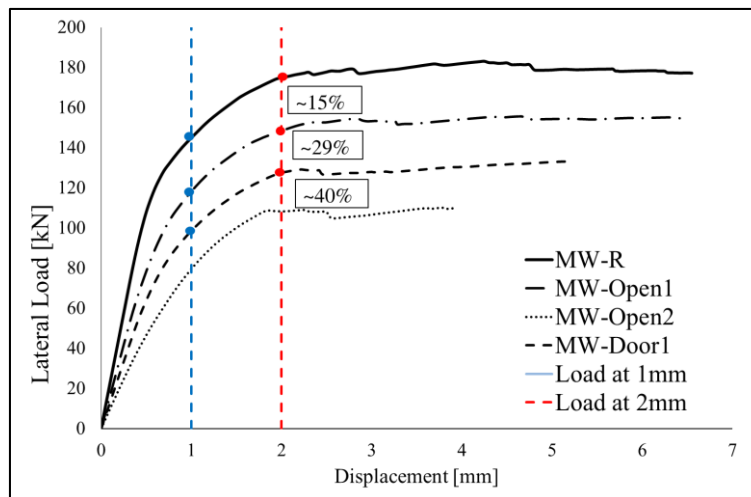

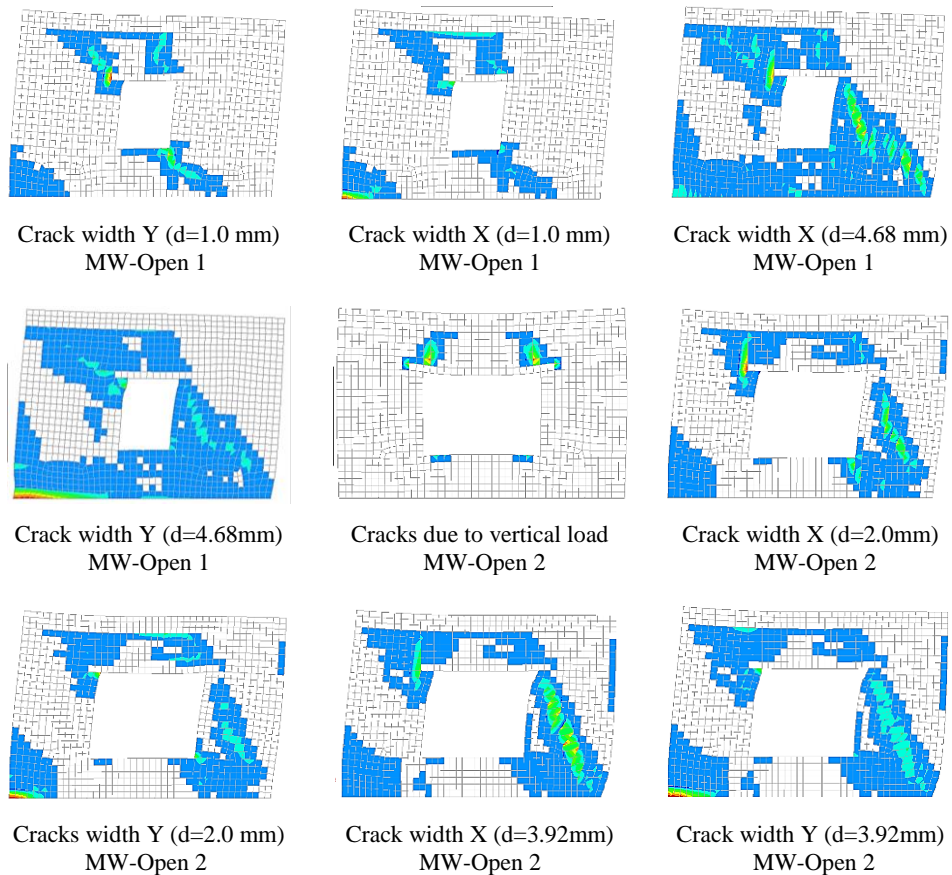Figure 7: Numerical Lateral Load – Displacement curves for the simulated walls

Crack width Y (d=1.0 mm)
MW-Open 1

Crack width X (d=1.0 mm)
MW-Open 1

Crack width X (d=4.68 mm)
MW-Open 1

Crack width Y (d=4.68mm)
MW-Open 1

Cracks due to vertical load
MW-Open 2

Crack width X (d=2.0mm)
MW-Open 2

Cracks width Y (d=2.0 mm)
MW-Open 2

Crack width X (d=3.92mm)
MW-Open 2

Crack width Y (d=3.92mm)
MW-Open 2

Figure 8: Crack patterns development for MW-Open1 and MW-Open2.

Crack width X (d=1.0mm)   Crack width Y (d=1.0mm)   Crack width X (d=2.6 mm)   Crack width Y (d=2.6 mm)
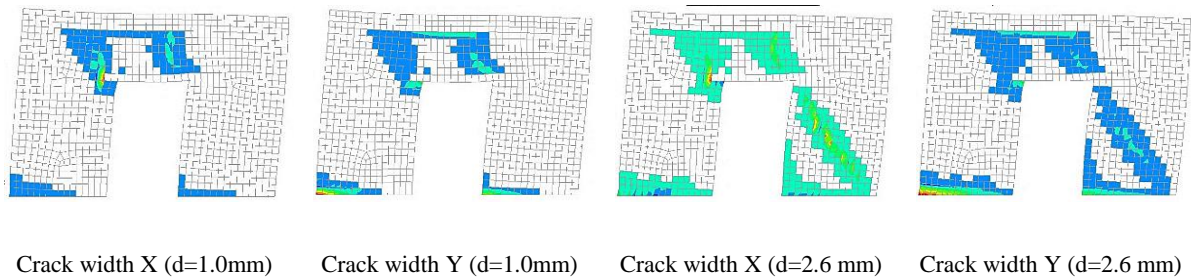
Figure 9: Crack patterns development for MW-Door 1.

3.3 Concluding remarks from numerical campaign

From Figure 7, it can be observed that the weakest wall is the one with the wider opening (MW-Open 2). MW-Door's performance seems to be in the middle of MW-Open 1 and MW-Open 2 when comparing initial stiffness and load carrying capacity. From Figure 8, it is observed that the masonry portion at the bottom of the openings does not experience any damage; therefore, the main aspect for the difference in stiffness and peak load is not in the height of opening but its length. For example, the response of MW-Open 1 is stiffer than the MW-Door, which has an opening length 210mm wider. At the same time MW-Door has a stiffer response than MW-Open 2, which has an opening 420mm wider than MW-Door (see geometry in Figure 2).

Since opening a door is the most common scenario in real practice and MW-Door model is one of the most vulnerable walls, the authors carried out an experimental test under cyclic quasi-static in-plane loading conditions on a wall with the characteristics of MW-Door. The overall response of this test is later compared with the numerical results.

4 EXPERIMENTAL PROGRAM: MW-DOOR

4.1 Materials, geometry, load and set up description

Materials, geometry, average vertical pressure and testing conditions were the same of MW-R [8] to be able to compare results between a squat wall (MW-R) and a wall with door opening (MW-Door). Solid clay bricks with dimensions of 240x110x50 [mm] were used and wall's dimensions are those from model MW-Door. The cutting-out process and the following in-plane test were carried out with maintaining a constant vertical load of 250kN, which introduces a pressure of 0.32MPa that corresponds to 5.3% of the masonry compressive strength (representative of a two-story masonry building). Load was kept constant by a hydraulic jack.

4.2 Cutting-out process for the new opening

As shown in Figure 10a, the original solid wall was placed in the loading set-up and loaded vertically. Then, a cut off saw of 90cm diameter was fixed to the wall to make two vertical cuts to define the door's borders. After these cuts, vertical props where placed to bear the vertical load when the masonry is taken out and replaced with the steel lintel (Figure 10b). The lintel consists in two profiles HEA120, connected by two M12 threaded rods, at each side of the profiles. The lintel was fixed to the wall with a surrounding mortar of fc=20MPa. The bedding area was 170mm x 250mm and 12 mm thickness (Figure 10c). Once the mortar was dried, the masonry in the bottom of the lintel and the supporting props were removed (Figure 10d).
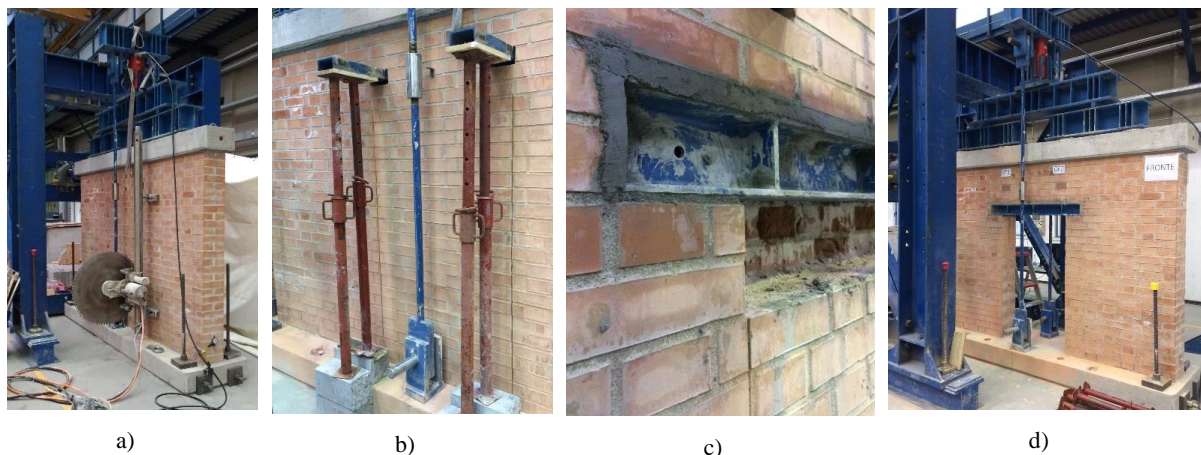

a)   b)   c)   d)

Figure 10: Sequence of the door's cutting-out process.

4.3 In-plane cyclic test

When the specimen was still under the vertical load, a lateral displacement history was applied to the top concrete beam by means of an electromechanical jack at a rate of 100μm/s. Details of the experimental testing set up, loading history and instrumentation are shown in Figure 11 and 12.
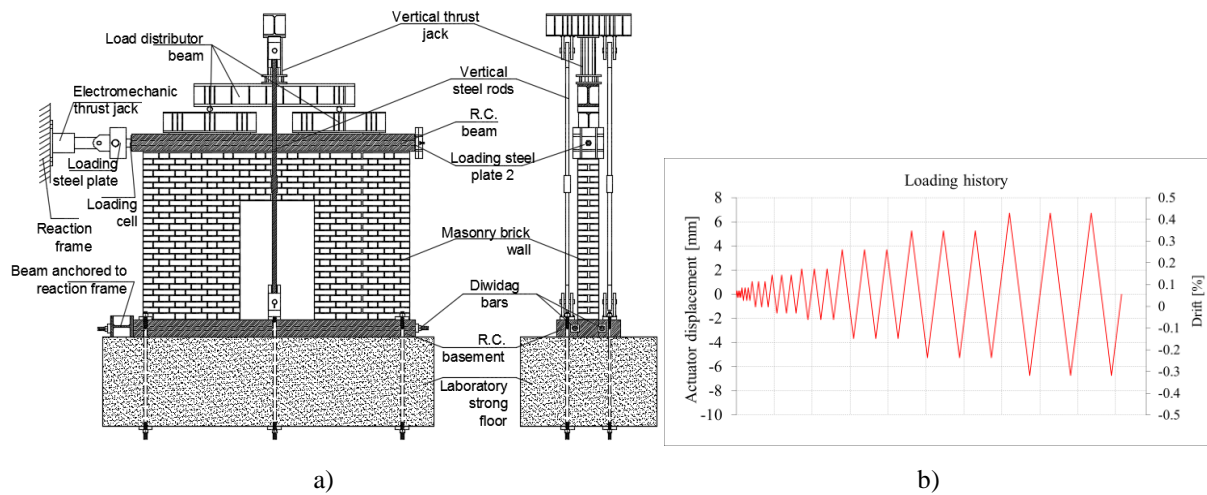
Figure 11: a) Elevation of experimental testing setup b) Loading history.
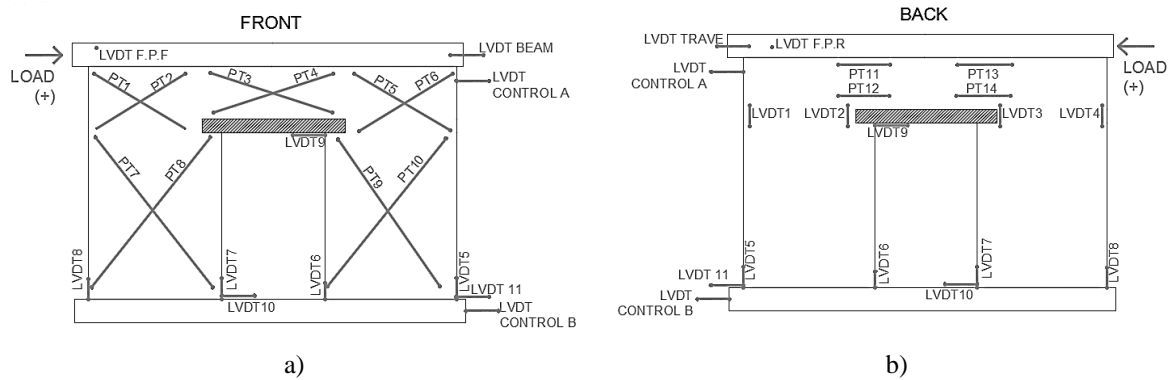

Figure 12: Layout of the instruments adopted for the test.

5 PRELIMINARY RESULTS FROM EXPERIMENTAL TESTS: MW-R VS MW-DOOR

5.1 Cracking patterns

Final cracks from experimental test are schematized in Figures 13a and 13b. Cracks started developing at a displacement of 1 mm *(drift=dr=0.05%)*. First cracks were horizontal and along the base and along *~h/2* of pier 2. A diagonal crack in pier 1 started from the left corner of the lintel and continued developing for the next cycles until *dr=0.25%*. The crack at *~h/2* of pier 2 continued until the last drift *dr= 0.32%,* at this point crack arrived to the bottom corner of the steel lintel. Cracks at the base of piers 1 and 2 started at *dr=0.05%* and finished at *dr=0.25%*. The spandrel had developed a mixed flexural-shear failure, with vertical cracks at the end of the lintel and stair-stepped shear crack in the spandrel. Finally, it was observed that all cracks were symmetrical when comparing back and front view, meanwhile cracks from pier 1 to pier 2 seemed asymmetrical. This is confirmed by the curves shown in Figure 14, where the wall seems to be stiffer when negative load is applied, and more flexible when loaded on the positive side. This might be due to a mechanism of collapse as shown in Figure 14c. Finally, the main failure mode observed during the test has involved rocking of both piers with flexural and shear cracks in the spandrel and sliding at mid-height of pier 2.

Since MW-R had very similar dimensions to MW-Door (3070mm x 2170mm x 250mm) and was tested under the same set-up and loading conditions, a comparison between cracking patterns and L-D response is possible. From the cracks observed in the squad wall MW-R (Figure 6) and the wall with opening (Figure 13), one can see that the failure mechanism has changed from mixed flexural/diagonal cracking to rocking/sliding behavior.
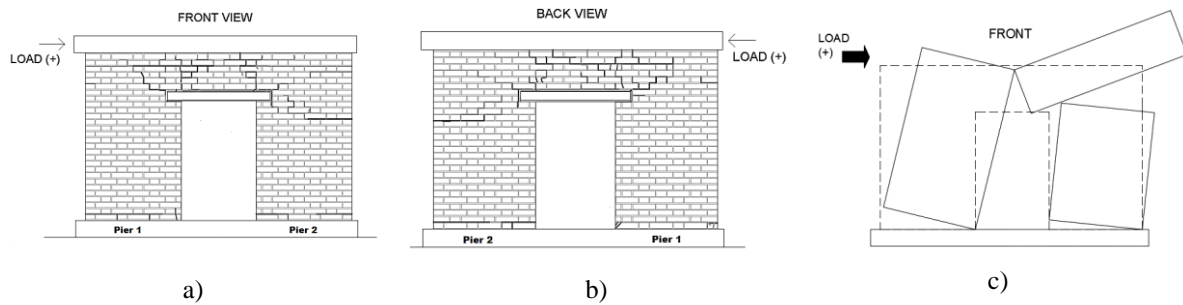

a)   b)   c)

Figure 13: a) and b) Cracking patterns from the experimental test; c) hypothesis of the mechanism of collapse.

5.2 Load carrying capacity

From Figure 16, it can be observed than MW-Door was much more deformable than MW-R and has presented about 50% reduction of the initial stiffness and a peak load decay of 40kN, which is about 24% with respect to the MW-R's peak load. These values are very close to the numerical prediction described in Section 3.2, where the initial stiffness from MW-R was 41% greater than MW-Door and peak load was 30% greater.

5.3 Experimental vs Numerical results

As observed in Figure 14, the numerical simulation with the calibrated values for the model parameters, valid for the MW-R, was not capable of predicting with accuracy the response of the wall with opening. For the positive direction of loading, the model overestimates the wall's response and is incapable of reproducing the stiffness degradation during the loading process. Meanwhile for the negative direction of loading, the model underestimates wall's load carrying capacity.
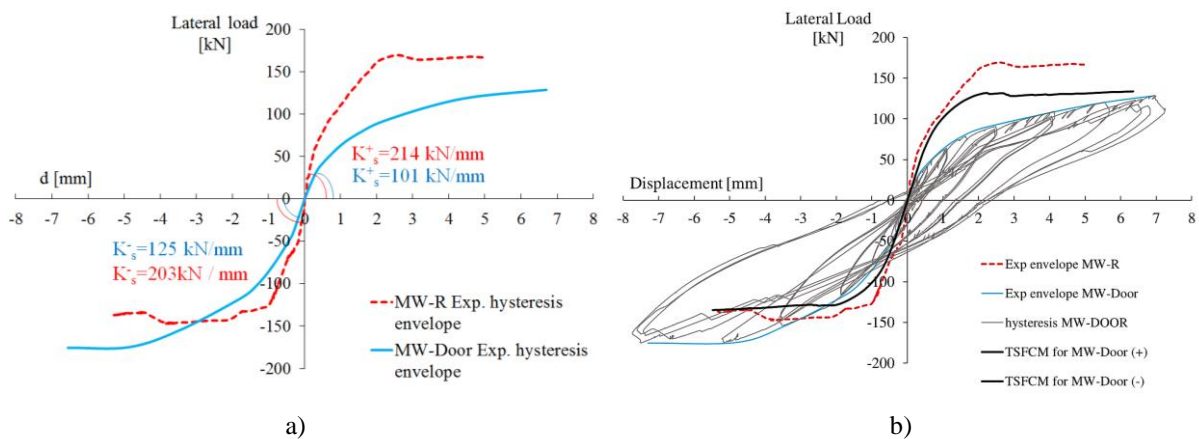

a)   b)

Figure 14. Results from experimental and numerical: squad wall (MW-R) vs wall with opening (MW-Door).

When cracking patterns predicted by the TSFCM are analyzed, it can be verified that the model generates some cracks in the spandrel, in the lintel's corner and along the wall's base. These cracks agree with the experimental cracking pattern. However, the model shows diagonal cracks, which were not present in the experimental. The TSFCM provides very good results for a squat wall under in-plane loading; however, for a wall with an irregular geometry, as it is the wall with opening results differ widely, stiffness is overestimated, and tensile strength and energy absorption is underestimated. A possible explanation is that, as sustained in [4], since total strain-based continuum models do not distinguish between tensile cracks (either normal to bed- or head-joints) and shear cracks, they might fail to accurately reproduce the different failure modes of masonry. Moreover, as in [3] the stiffness until the point of cracking is assumed to be equal in compression and tension and for low values of precompression levels, this can be a source of error.

6   FINAL REMARKS

- the presence of a new opening in an unreinforced masonry wall can significantly change the failure mode of the wall when in-plane loading is applied.

- Numerical models show that wider openings are the most vulnerable case scenario. Height of the openings might not be relevant, but opening's length can have a higher impact in the wall's performance.

- From the registered experimental L-D curves, it is seen that a wall with door opening is much more flexible than a squat wall, the initial stiffness of this specimen has decreased in about 50% and the peak load in about 40% with respect to the squat wall.

- Experimental crack patterns suggest that while squat wall has failed in a mixed flexural/diagonal cracking, the wall with a door opening has experienced a rocking/sliding type failure.

- When comparing the numerical prediction with the experimental behavior of squat wall and wall with an opening, it was found that the adopted TSFCM is capable of providing good results for the squad wall but not for the wall with a door opening.

- As in [3], numerical simulations with TSFCM did not fit accurately the initial stiffness and ductility level registered experimentally, therefore the authors are intended to explore the potentialities of a dedicated model to masonry systems, described in [4], in the following steps of this research project.

7   ACKNOWLEDGEMENTS

REFERENCES

[1]   P. Medeiros, G. Vasconcelos, P.B. Lourenco, J. Gouveia, Numerical modelling of non-confined and confined masonry walls. *Construction and Building Materials*; **41**, 968-976, 2013.

[2] J.R. Van Noort, *Computational modelling of masonry structures.* Master Thesis, Delft University Press, Delft (NL), 2013.

[3] C. Allen, M. Masia, A. Page, M. Griffith, J. Ingham, Nonlinear finite element modelling of unreinforced masonry walls with opening subjected to in-plane shear. *13th Canadian Masonry Symposium.* Halifax, Canada. June 4th – 7th, 2017.

[4] TNO *DIANA, Diana user's manual. Release 9.4.3, 2010.*

[5] J.G. Rots, F. Messali, R. Esposito, S. Jafari, V. Mariani, Computational modelling of masonry with a view to Groeningen induced seismicity. *10th International Conference on Structural Analysis of Historical Construction SAHC.* September 13th -15th, 2016.

[6] P.B. Lourenco, J.G. Rots, J. Blaauwendraad, Continuum model for masonry: parameter estimation and validation. *Journal Structural Engineering, ASCE*, **124** (6), 642-52, 1998.

[7] G. Milani, P.B. Lourenco, A. Trali, Homogenized limit analysis of masonry walls. Part I: failure surfaces. *Journal Computer & Structures*; **84** (3-4): 166-80, 2006.

[8] L. Facconi, *Fiber Reinforced Concrete and Mortar for enhanced structural elements and structural repair of masonry walls*, PhD Thesis, Università degli Studi di Brescia. 2013.

[9] D.A. Hordijk, *Local approach to fatigue of concrete*. PhD Thesis, Delft University of Technology, Delft University Press, Delft (NL), 1991.

[10] J. Hoshikuma, K. Kawashima, K. Nagaya and A. W. Taylor. Stress-strain model for reinforced concrete in bridge piers. *Journal Structural Engineering ASCE*, **120:1** (63), 63-81, 1994.

[11] P.H. Feenstra, *Computational aspects of biaxial stress in plain and reinforced concrete.* PhD thesis, Delft University of Technology, Delft University Press, Delft (NL), 1993.

[12] F.J., Vecchio, and M. P. Collins. The modified compression field theory for reinforced concrete elements subjected to shear. *ACI Journal* **83** (22) 219-231, 1986.

[13] F.J. Vecchio, Disturbed stress field model for reinforced concrete: formulation, *Journal Structural Engineering ASCE,* **126** (9), 1070-1077, 2000.

[14] L. Facconi, G. Plizzari, F. Vecchio, Disturbed Stress Field Model for Unreinforced Masonry. *Journal Structural Engineering* **140**, Issue 4, April 2014.